Structure, Stability, and Interconversion Barriers of the Rotamers of *cis*-[$Pt^{II}Cl_2$(quinoline)$_2$] and *cis*-[$Pt^{II}Cl_2$(3-bromoquinoline)(quinoline)] from X-ray Crystallography, NMR Spectroscopy and Molecular Mechanics Evidence

Murray S. Davies, Connie I. Diakos, Barbara A. Messerle,† and Trevor W. Hambley*

Centre for Heavy Metals Research, School of Chemistry, University of Sydney, Sydney, NSW 2006, Australia

Received September 29, 2000

Reported are the preparations of *cis*-[$PtCl_2$(quinoline)$_2$] and *cis*-[$PtCl_2$(3-bromoquinoline)(quinoline)] and an investigation of the stabilities and interconversion of the rotamer forms of these complexes. Both *head-to-head* (HTH) and *head-to-tail* (HTT) rotamer forms are found in the crystal structure of *cis*-[$PtCl_2$(quinoline)$_2$]. The NOESY NMR spectrum of *cis*-[$PtCl_2$(quinoline)$_2$] in dmf-d_7 at 300 K is consistent with conformational exchange brought about by rotation about the Pt−N(quinoline) bonds. H···H nonbonded distances between H atoms of the two different quinoline ligands were determined from NOESY data, and these distances are in accord with those observed in the crystal structure and derived from molecular mechanics models. *cis*-[$PtCl_2$(3-bromoquinoline)-(quinoline)] was prepared to alleviate the symmetry-imposed absence of inter-ring H2/H2 and H8/H8 NOESY cross-peaks for *cis*-[$PtCl_2$(quinoline)$_2$]. Molecular mechanics calculations on the complexes show the HTT rotamers to be 1−2 kJ mol^{-1} more stable than the HTH forms, consistent with the ^{1}H spectra where the intensities of resonances for the two forms are approximately equal. Variable-temperature ^{1}H NMR spectra of *cis*-[$PtCl_2$-(quinoline)$_2$] in dmf-d_7 indicate a rotational energy barrier of 82 ± 4 kJ mol^{-1}. Variable-temperature ^{1}H NMR spectra indicate that the Br substituent on the quinoline ring does not affect the energy barrier to interconversion between the HTT and HTH forms (79 ± 5 kJ mol^{-1}). The steric contribution to the rotation barrier was calculated using molecular mechanics calculations and was found to be ∼40 kJ mol^{-1}, pointing to a possible need for an electronic component to be included in future models.

Introduction

The importance of the bifunctional DNA adducts formed by Pt anticancer agents has generated great interest in the structural properties of bis(purine)platinum(II) complexes.[1−19] Such complexes may exist as two rotamers, generally referred to as head-to-head (HTH) and head-to-tail (HTT) (Scheme 1), and both the relative stabilities of these rotamers and the energy barrier to interconversion between them have been extensively studied.[3,4,7−9,11,13,20]

The HTT form of *cis*-[$Pt(NH_3)_2(Pu)_2$] (Pu = purine) exists as two enantiomers differing in the screw sense about the bisector of the N7(purine)−Pt−N7(purine) angle. NMR experiments reveal rapid interconversion between these diastereomers, especially when the purine is guanine.[2,6] Studies carried out on complexes with bulky amine ligands trans to the purines showed slowed interconversion between the HTH and HTT forms.[1,3,4,10] Cramer and Dahlstrom[1] determined an energy barrier of ∼86 kJ mol^{-1} for *cis*-[$Pt(Guo)_2(TMEDA)]^{2+}$ (TMEDA = *N*,*N*,*N*′,*N*′-tetramethylethylenediamine; Guo = guanosine) in aqueous solution. The same authors[6] obtained energy barriers for the different diastereomeric forms of *cis*-[Pt(*N*,*N*′-dimethylethylenediamine)$(Guo)_2]^{2+}$ in the range 57−65 kJ mol^{-1}.

Stang et al.[21] used ^{31}P NMR to study rotation about Pt−N in a number of bis(quinoline) and bis(isoquinoline) complexes with

* Corresponding author. Ph: 61-2-9351-2830. Fax: 61-2-9351-3329. E-mail: t.hambley@chem.usyd.edu.au.

† Present address: School of Chemistry, University of NSW, Kensington, Sydney, NSW 2052, Australia.

(1) Cramer, R. E.; Dahlstrom, P. L. *J. Am. Chem. Soc.* **1979**, *101*, 3679−3681.
(2) Cramer, R. E.; Dahlstrom, P. L.; Seu, M. J. T.; Norton, T.; Kashiwagi, M. *Inorg. Chem.* **1980**, *19*, 148−154.
(3) Gullotti, M.; Pacchioni, G.; Pasini, A.; Ugo, R. *Inorg. Chem.* **1982**, *21*, 2006−2014.
(4) Marcelis, A. T. M.; van der Veer, J. L.; Zwetsloot, J. C. M.; Reedijk, J. *Inorg. Chim. Acta* **1983**, *78*, 195−203.
(5) Dijt, F. J.; Canters, G. W.; den Hartog, J. H. J.; Marcelis, A. T. M.; Reedijk, J. *J. Am. Chem. Soc.* **1984**, *106*, 3644−3647.
(6) Cramer, R. E.; Dahlstrom, P. L. *Inorg. Chem.* **1985**, *24*, 3420−3424.
(7) Reily, M. D.; Marzilli, L. G. *J. Am. Chem. Soc.* **1986**, *108*, 6785−6793.
(8) Marcelis, A. T. M.; Korte, H.-J.; Krebs, B.; Reedijk, J. *Inorg. Chem.* **1982**, *21*, 4059−4063.
(9) Hambley, T. W. *Inorg. Chem.* **1988**, *27*, 1073−1077.
(10) Kiser, D.; Intini, F. P.; Xu, Y.; Natile, G.; Marzilli, L. G. *Inorg. Chem.* **1994**, *33*, 4149−4158.
(11) Xu, Y.; Natile, G.; Intini, F. P.; Marzilli, L. G. *J. Am. Chem. Soc.* **1990**, *112*, 8177−8179.
(12) Ano, S. O.; Intini, F. P.; Natile, G.; Marzilli, L. G. *J. Am. Chem. Soc.* **1997**, *119*, 8570−8571.
(13) Williams, K. M.; Cerasino, L.; Intini, F. P.; Natile, G.; Marzilli, L. G. *Inorg. Chem.* **1998**, *37*, 5260−5268.
(14) Navarro, J. A. R.; Salas, J. M.; Romero, M. A.; Vilaplana, R.; Gonzalez-Vilchez, F.; Faure, R. *J. Med. Chem.* **1998**, *41*, 332−338.
(15) Lippert, B.; Raudaschl, G.; Lock, C. J. L.; Pilon, P. *Inorg. Chim. Acta* **1984**, *93*, 43−50.
(16) Schollhorn, H.; Raudaschl-Sieber, G.; Muller, G.; Thewalt, U.; Lippert, B. *J. Am. Chem. Soc.* **1985**, *107*, 5932−5937.
(17) Kirstenmacher, T. J.; Chiang, C. C.; Chalilpoyil, P.; Marzilli, L. G. *J. Am. Chem. Soc.* **1979**, *101*, 1143−1148.
(18) Marzilli, L. G.; Chalilpoyil, P.; Chiang, C. C.; Kirstenmacher, T. J. *J. Am. Chem. Soc.* **1980**, *102*, 2480−2482.
(19) Gellert, R. W.; Bau, R. *J. Am. Chem. Soc.* **1975**, *97*, 7379−7380.
(20) Li, D.; Bose, R. N. *J. Chem. Soc., Dalton Trans.* **1994**, 3717−3721.
(21) Stang, P. J.; Olenyuk, B.; Arif, A. M. *Organometallics* **1995**, *14*, 5281−5289.

10.1021/ic001278v CCC: $20.00
Published on Web 05/17/2001

Scheme 1. Head-to-Head and Head-to-Tail Forms of *cis*-[$PtCl_2$(quinoline)$_2$] and *cis*-[$PtCl_2$(3-bromoquinoline)-(quinoline)] Showing the Numbering Scheme Used in the NMR Analysis

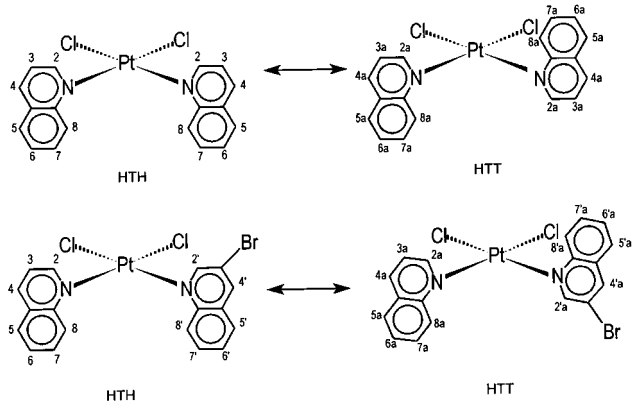

a $Pt(PR_3)_2$ moiety. Different ^{31}P shifts for the phosphine ligands were found for the HTH and HTT isomers, and a rotational energy barrier in excess of 70 kJ mol^{-1} was determined. The X-ray crystal structure obtained of [Pt(dppp)(quinoline)$_2$](OTf)$_2$ (dppp = (diphenylphosphino)propane; OTf = triflate) showed the quinoline rings disposed in a HTH arrangement. Further, it was shown that there is no equilibrium between the isomers of this particular complex, as recrystallization resulted in an increased proportion of the HTH rotamer. Rochon et al.[22] have shown that the barrier to rotation in *trans*-[$PtCl_2$(2-methylpyridine)$_2$] is greater than 71 kJ mol^{-1}.

It is clear from these studies that interligand interactions of various types influence both the isomer distribution and rotational energy barriers, but it is not clear what types of interactions are most important nor is it clear whether there is a significant electronic component to the rotational energy barrier. In the present study we have sought to answer some of these questions using a system free of the complications present in many of the earlier studies namely *cis*-[$PtCl_2$(quinoline)$_2$] and *cis*-[$PtCl_2$(3-bromoquinoline)(quinoline)]. Quinoline type ligands were chosen as purine substitutes because they are similar structurally to the purines and are planar but lack groups capable of forming strong hydrogen bonds with other ligands about the Pt atom. In addition, quinoline H8 and H2 interactions can be monitored using ^1H NMR spectroscopy. Quinoline complexes and their structural properties are themselves of interest because some exhibit anticancer activity.[23−27] We present the crystal structures and NMR studies of structure and rotation of the quinolines about the Pt−N bond.

Experimental Section

Instrumentation. Infrared spectra of the complexes dispersed in KBr were recorded on a Biorad FTS-40 Fourier transform infrared spectrometer using the diffuse reflectance method. Elemental analyses were carried out at the Microanalytical laboratory in the Research School of Chemistry at the Australian National University.

Preparation of *cis*-[$PtCl_2$(quinoline)$_2$]. $K_2[PtCl_4]$ (0.233 g, 0.561 mmol) in H_2O (2.5 mL) and quinoline (0.145 g, 1.12 mmol) in EtOH (2.5 mL) were stirred at 310 K for 24 h. The reaction was initially hastened by sonicating the solution. The solution became cloudy orange and appeared biphasic. Over time the solution color faded as a yellow powder formed. The suspension was filtered off and the residue rinsed with water, MeOH, and Et_2O to give *cis*-[$PtCl_2$(quinoline)$_2$] as a yellow solid (0.191 g, 0.363 mmol, 65%). The complex was recrystallized from warm dimethylformamide to give prisms suitable for X-ray diffraction. IR (KBr; cm^{-1}): 3069 s, 3040 sh, 3015 sh, 1675 w, 1619 w, 1589 w,1508 vs, 1459 w,1437 vw, 1393 w, 1372 w, 1309 wm, 1261 w, 1209 w, 1151 w, 1129 w, 1063 vw, 1019 w, 874 w, 815 ms, 787 sh, 779 s, 745 w, 644 w, 534 vw, 522 w, 515 w, 506 w, 468 w, 410 w. ^1H NMR (dmf-d_7, δ, ppm): 10.22 H8a (d, ^3J = 5.0 Hz), 10.05 H8 (d, ^3J = 5.0 Hz), 9.89 H2 (d, ^3J = 5.6 Hz), 9.71 H2a (d, ^3J = 5.6 Hz), 8.69 H4/H4a (dd, ^3J = 8.4 Hz), 8.17 H7a (dd, ^3J = 7.2 Hz), 8.10 H5 (dd), 8.05 H7/H5a (dd, $^3J \sim$ 7.6 Hz), 7.79 H6 (dd, ^3J = 7.6 Hz), 7.72 H3a (dd, ^3J = 7.6 Hz), 7.68 H6a (dd, ^3J = 5.6 Hz), 7.55 H3 (dd, ^3J = 6.4 Hz). Anal.Calcd for $PtCl_2C_{18}H_{14}N_2{\cdot}0.25C_3H_7NO$: C, 41.50; H, 2.92; N, 5.80. Found: C, 41.54; H, 3.00; N, 5.95.

Preparation of *cis*-[$PtCl_2$(3-bromoquinoline)(quinoline)]. $K_2[PtCl_4]$ (0.255 g, 0.614 mmol) and 3-bromoquinoline (0.129 g, 0.620 mmol) were stirred overnight at ~330 K in dimethylformamide (dmf) (20 mL) according to the procedure of Kong and Rochon.[28] After KCl was filtered off, the clear orange-yellow solution, on concentration, precipitated K[$PtCl_3$(3-bromoquinoline)] as a yellow solid (0.271 g, 0.495 mmol, 80%). The solid was washed with H_2O (1 mL), EtOH (2 mL), and Et_2O (5 mL) and was dried at the pump. IR (KBr; cm^{-1}): 3081 m, 3062 m, 2074 w, 1666 m, 1574 m, 1499 vs, 1451 mw, 1371 m, 1362 m, 1307 w, 1274 w, 1231 w, 1185 w, 1180 w, 1149 w, 1139 ms, 1095 m, 971 ms, 894 ms, 865 m, 850 m, 788 w, 775 s, 756 ms, 622 w, 588 mw, 559 w, 504 m, 437 mw. K[$PtCl_3$(3-bromoquinoline)] (0.163 g, 0.297 mmol) and quinoline (0.035 g, 0.297 mmol) were stirred overnight in a mixture of EtOH (2.5 mL), H_2O (2.5 mL), and dmf (5 mL). A yellow solid was obtained, and the presence of both quinoline and 3-bromoquinoline ligands was confirmed by IR and NMR analysis. IR (KBr; cm^{-1}): 3057 s, 3014 sh, 1670 m, 1619 vw, 1575 m, 1508 vs, 1498 s sh, 14571 w, 1437 vw, 1393 w, 1371 m, 1359 sh, 1307 ms, 1294 sh, 1262 w, 1232 w, 1208 m, 1191 w, 1152 m, 1133 m, 1127 sh, 1094 m, 1020 w, 974 m, 964 m, 936w, 900 ms, 861 mw, 851 m, 820s, 776 s, 754s. ^1H NMR (dmf-d_7, δ, ppm): 10.25 H8 (d, ^3J = 8.8 Hz), 10.19 H8′a (d, ^3J = 8.8 Hz) 10.09 H2′(s), 10.02 H8a/H8′ (d, ^3J = 8.4 Hz), 9.99 H2 (d, ^3J = 4.8 Hz), 9.89 H2′a (s), 9.71 H2a (d, ^3J = 4.8 Hz), 8.96 H4′a (s), 8.90 H4 (d, ^3J = 10.4 Hz), 8.73 H4′ (s), 8.57 H4/H4a (dd, ^3J = 12.6 Hz), 8.12 H7/H7a (dd, ^3J = 12.6 Hz), 8.12 H7′a (dd, ^3J = 12.6 Hz), 8.06, 8.05, 8.03, 8.00 H7′/H5/H5′/H5′a/H5a (complex overlap of resonances), 7.77, 7.75, 7.73, 7.71, 7.70, 7.68, 7.66 H6/H3/H6′/H6′a (complex overlap of resonances), 7.55 H3a (dd, ^3J = 12.6 Hz), Anal. Calcd for $PtBrCl_2C_{18}H_{13}N_2$: C, 35.84; H, 2.17; N, 4.64. Found: C, 35.94; H, 2.06; N, 4.56. The product can also be obtained by exchanging the order of substitution. Thus, addition of 1 equiv of quinoline to $K_2[PtCl_4]$ in dimethylformamide under identical conditions yields K[$PtCl_3$(quinoline)]. IR (KBr;cm^{-1}): 3075 m, 3052 m, 3016 mw, 1992 w, 1912 w, 1853 w, 1829 w, 1771 w, 1652 w, 1621 w, 1592 w, 1510 vs, 1461 m, 1438 w, 1397 m, 1374 w, 1311 m, 1374 m, 1311 m, 1268 m, 1207 w, 1153 mw, 1146 mw, 1131 m, 1100 w, 1074 w, 1019 w, 1000 w, 986 m, 965 m, 874 w, 821 vs, 808 vs, 774 vs, 685 w, 657 m, 626 w, 515 w, 503 m, 470 w, 415 wm.

Crystallography. A crystal of *cis*-[$PtCl_2$(quinoline)$_2$] of dimensions 0.25 × 0.15 × 0.10 mm was selected and mounted onto a glass fiber. Crystal data and experimental details are summarized in Table 1. Data were collected at 294 K, and cell constants were determined by a least-squares fit to the setting parameters of 25 independent reflections, measured and refined on an Enraf-Nonius CAD4-F diffractometer with graphite-monochromated Mo Kα (λ = 0.710 69 Å) radiation. Data reduction and application of Lorentz, polarization, and analytical absorption corrections were carried out using teXsan.[29] The structure

(22) Rochon, F. D.; Beauchamp, A. L.; Bensimon, C. *Can. J. Chem.* **1996**, *74*, 2121−2130.
(23) Van Beusichem, M.; Farrell, N. *Inorg. Chem.* **1992**, *31*, 634−639.
(24) Bierbach, U.; Qu, Y.; Hambley, T. W.; Peroutka, J.; Nguyen, H. L.; Doedee, M.; Farrell, N. *Inorg. Chem.* **1999**, *38*, 3535−3542.
(25) Kharatishvili, M.; Mathieson, M.; Farrell, N. *Inorg. Chim. Acta* **1997**, *255*, 1−6.
(26) Bierbach, U.; Farrell, N. *J. Biol. Inorg. Chem.* **1998**, *3*, 570−580.
(27) Bierbach, U.; Farrell, N. *Inorg. Chem.* **1997**, *36*, 3657−3665.
(28) Kong, P.-C.; Rochon, F. D. *J. Chem. Soc., Chem. Commun.* **1975**, 599−600.
(29) *teXsan, Crystal Structure Analysis Package*; Molecular Structure Corp.: The Woodlands, TX, 1985, 1992.

Table 1. Crystal Data and Experimental Details for *cis*-[$PtCl_2$(quinoline)$_2$]

space group	*C*2/*c* (No. 15)
a, Å	29.05(1)
b, Å	12.046(5)
c, Å	16.584(5)
β, deg	101.90(3)
V, Å^3	5679(4)
fw	524.4
empirical formula	$C_{18}H_{14}Cl_2N_2Pt\cdot 0.25$dmf
Z	12
μ, cm^{-1}	76.66
transm coeffs	0.443−0.630
ρ_{obsd}, g cm^{-3}	1.840
temp, °C	21
λ, Å	0.710 69
$R(F_o)$	0.056
R_w	0.046

Table 2. Selected Bond Lengths (Å) and Angles (deg) for *cis*-[$PtCl_2$(quinoline)$_2$][a]

Pt(1)−N(1)	2.02(1)	Pt(1)−Cl(1)	2.289(4)
Pt(1)−N(2)	2.04(1)	Pt(1)−Cl(2)	2.288(4)
Pt(2)−N(3)	2.07(1)	Pt(2)−Cl(3)	2.276(5)
Cl(1)−Pt(1)−Cl(2)	92.1(2)	Cl(1)−Pt(1)−N(2)	179.3(4)
Cl(1)−Pt(1)−N(1)	89.0(3)	Cl(2)−Pt(1)−N(1)	176.8(4)
Cl(2)−Pt(1)−N(2)	87.3(4)	N(1)−Pt(1)−N(2)	91.7(5)
Cl(3)−Pt(2)−Cl(3)^i	91.5(3)	Cl(3)−Pt(2)−N(3)^i	179.2(4)
N(3)−Pt(2)−N(3)^i	92.0(7)		

[a] i = $-x$, y, 1/2 − z.

was solved by direct methods using SHELXS-86[30] and refined using full-matrix least-squares methods with teXsan.[29] Hydrogen atoms were included at calculated sites with thermal parameters derived from the parent atoms. Non-hydrogen atoms were refined anisotropically. Scattering factors and anomalous dispersion terms for Pt were taken from ref 31. Anomalous dispersion effects were included in F_c;[32] the values for $\Delta f'$ and $\Delta f''$ were those of Creagh and McAuley.[33] The values for the mass attenuation coefficients are those of Creagh and Hubbell.[34] All other calculations were performed using the teXsan[29] crystallographic software package of Molecular Structure Corp. Selected bond lengths and angles are listed in Table 2. The atomic nomenclature is defined on the ORTEP[35] plots of both rotamer forms of *cis*-[$PtCl_2$(quinoline)$_2$] in Figure 1. Listings of atom coordinates and complete tables of bond lengths and angles, anisotropic thermal parameters, and details of least-squares-planes calculations have been deposited and are given as Supporting Information.

NMR Experiments. NMR spectra of *cis*-[$PtCl_2$(quinoline)$_2$] in dmf-d_7 were recorded on a Bruker DRX 400 MHz spectrometer. ^{1}H spectra were recorded at 10 K intervals in the temperature range 215−365 K and were referenced against the residual ^{1}H resonances of the solvent. Temperatures were calibrated against MeOH and ethylene glycol in the appropriate ranges for these solvents.[36] Two-dimensional spectra were acquired in phase-sensitive mode using time-proportional phase incrementation. NOESY and COSY spectra were obtained at 300 K, a NOESY spectrum was also obtained at 215 K, and the spectra were collected using standard Bruker pulse sequences. The COSY spectrum was collected over a spectral width of 4400 Hz, with 512 increments of t_1 acquired which were zero filled to 1024 points, with each free induction decay (FID) composed of 2048 data points. For each increment of t_1 4 transients were recorded with the recycle delay of 1.8 s. The NOESY spectra were acquired with a mixing time (τ_m) of 1.2 s, over a spectral width of 3900 Hz. The 800 increments of t_1 were acquired with zero filling to 1024 points, with each FID composed of 2048 data points. For each increment of t_1 16 transients were recorded with a recycle delay of 1.9 s. NOESY and COSY NMR spectra of *cis*-[$PtCl_2$(3-bromoquinoline)(quinoline)] in dmf-d_7 were recorded on a Bruker AMX 600 MHz spectrometer at 240 K. The NOESY spectrum was acquired over a spectral width of 6600 Hz with a mixing time of 1.2 s. A data set resulting from 720 increments of t_1 was acquired and zero filled to 1024 points, with each FID composed of 2048 data points. For each increment of t_1, 16 transients were recorded with a recycle delay of 2.5 s. Variable-temperature ^{1}H NMR spectra were recorded at 10 K intervals between 230 and 390 K on a Bruker DRX 400 MHz NMR spectrometer; in the 300−350 K region spectra were recorded every 5 K.

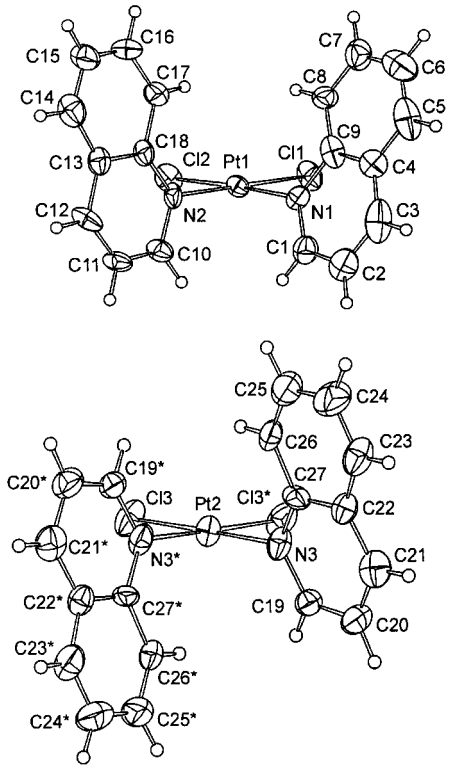

Figure 1. ORTEP plots of the two independent complex molecules of *cis*-[$PtCl_2$(quinoline)$_2$] giving the crystallographic atom numbering with 30% probability ellipsoids shown.

Line shape analyses were carried out using the XSIM program.[37] Data were then subjected to an Arrhenius analysis using the SCIENTIST program (version 2.01, MicroMath Inc.). NOESY peak intensities were determined by measuring peak volumes using standard Bruker software. Distances between nuclei were calculated using the formula $I = kr^{-6}$, where I is the intensity of the NOESY cross-peak, r is the distance between the nuclei responsible for the peak, and k is a constant of proportionality determined by comparison between vicinal H3/H4 cross-peak intensities and the known H3···H4 distance of 2.37 Å.

Molecular Mechanics Calculations. Molecular mechanics calculations were carried out using MOMECPC/HyperChem.[38] Starting models were generated and final models were viewed and analyzed using

(30) Sheldrick, G. M. In *SHELXS-86*; Sheldrick, G. M., Kruger, C., Goddard, R., Eds.; Oxford University Press: New York, 1986; pp 175−189.
(31) Cromer, D. T.; Waber, J. T. *International Tables for X-ray Crystallography*; Kynoch Press: Brimingham, U.K., 1974; Vol. 4.
(32) Ibers, J. A.; Hamilton, W. C. *Acta Crystallogr.* **1964**, *17*, 781.
(33) Creagh, D. C.; McAuley, W. J. *International Tables of Crystallography*; Kluwer Academic Publishers: Boston, MA, 1992; Vol. C, Tables 4.2, 4.3.
(34) Creagh, D. C.; Hubbell, J. H. *International Tables for Crystallography*; Kluwer Academic Publishers: Boston, MA, 1992; Vol. C.
(35) Johnson, C. K. *ORTEP, A Thermal Ellipsoid Plotting Program*; Oak Ridge National Laboratories: Oak Ridge, TN, 1965.
(36) Gunther, H. *NMR Spectroscopy-Basic Principles, Concepts and Applications in Chemistry*, 2nd ed.; Wiley and Sons: Chichester, U.K., 1998.
(37) Marat, K. *Xsim*; *X-11 motif Version 970501*; The University of Manitoba: Winnepeg, Manitoba, Canada, 1997.
(38) Comba, P.; Hambley, T. W.; Okon, N. *MOMEC-A Program for Molecular Mechanics Modelling of Metal Complexes*; Altenhoff and Schmitz: Dortmund, Germany, 1995.

HyperChem version 4.5.[39] Strain energies were minimized using MOMECPC.[38] Refinement was continued until all shifts were less than 0.001 Å. Constraints were applied using the method of Lagrangian multipliers.[40]

Results

Preparation of Complexes and X-ray Crystal Structure of *cis*-[PtCl$_2$(quinoline)$_2$]. *cis*-[PtCl$_2$(quinoline)$_2$] was prepared by reaction of K$_2$[PtCl$_4$] with 2 equiv of quinoline in a mixture of water and ethanol (1:1) with the ethanol used to solubilize the quinoline in the aqueous solution. Over 1 day at 310 K *cis*-[PtCl$_2$(quinoline)$_2$] forms as a yellow solid. The synthesis of *cis*-[PtCl$_2$(3-bromoquinoline)(quinoline)] was first attempted by reacting *cis*-[PtCl$_2$(dmso)$_2$] with 1 equiv of quinoline to form *cis*-[PtCl$_2$(dmso)(quinoline)],[23] but treatment of this species with 3-bromoquinoline failed to produce the desired complex, replacement of the remaining coordinated dmso ligand proving impossible. Instead, the method of Kong and Rochon[28] was used; reaction of K$_2$[PtCl$_4$] with 1 equiv of 3-bromoquinoline in dmf at ∼330 K afforded the complex K[PtCl$_3$(3-bromoquinoline)] as a yellow solid. Treatment of this species with 1 equiv of quinoline in a mixture of water, ethanol, and dmf afforded *cis*-[PtCl$_2$(3-bromoquinoline)(quinoline)] as a yellow solid in 80% yield. The reaction also gives the same product if the 3-bromoquinoline and quinoline are exchanged in the reaction scheme.

The X-ray crystal structure of *cis*-[PtCl$_2$(quinoline)$_2$] is remarkable in that it contains both HTH and HTT rotamer forms, and the ORTEP plots of both forms are shown in Figure 1. The structure consists of two independent neutral complex molecules and a disordered solvate molecule assigned as *N*,*N*-dimethylformamide. Subsequent and independent preparations afforded crystals with the same unit cell. Contacts between the molecules are indicative of hydrophobic interactions. One of the complex molecules is located at a general site and has a HTH arrangement of the quinoline ligands. The other is located with the Pt atom lying on a 2-fold axis and has an HTT arrangement of the quinoline ligands. The quinoline ligands are planar to within 0.06 Å, and the coordination planes, planar to within 0.03 Å. In all cases the quinoline ligands are canted with respect to the perpendicular to the coordination planes by 11−16° but the direction of the canting differs. Thus, in the HTH isomer the H8 atoms are canted toward the chloro ligands and away from each other resulting in a short H2···H2 contact (2.36 Å) and a longer H8···H8 separation (2.60 Å). The canting angles from the perpendicular are −16(1) and 11(1)°; thus, an approximate mirror plane passing through the Pt atom relates the two quinoline ligands. In the HTT isomer the H8 atoms are canted away from the chloro ligands. The canting angle is 12(1)° from the perpendicular, and the H2···H8 separation is 2.54 Å. In both molecules there are close contacts between the Pt and H8 atoms (HTH 2.73 and 2.76 Å; HTT 2.68 Å), and these result in an opening of 2−4° in the Pt−N−C angle closest to the H8 atoms.

NMR Spectra. The labeling scheme for the different rotamers of *cis*-[PtCl$_2$(quinoline)$_2$] and *cis*-[PtCl$_2$(3-bromoquinoline)(quinoline)] used in the assignment of the ^{1}H and NOESY spectra is shown in Scheme 1. The ^{1}H NMR spectra, deposited as Figure S6, were assigned using COSY and NOESY cross-peaks between neighboring protons in the quinoline rings. Large downfield shifts are found for the H2, H4, and H8 resonances relative to free quinoline and 3-bromoquinoline.[41]

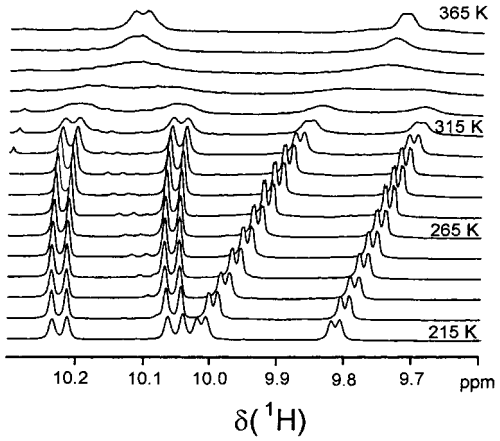

Figure 2. Temperature dependence of the ^{1}H NMR spectrum of *cis*-[PtCl$_2$(quinoline)$_2$] in dmf-d_7.

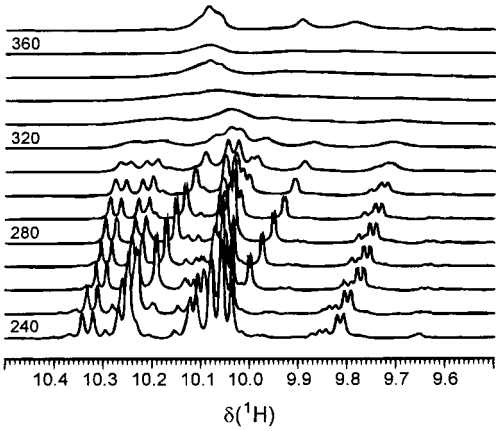

Figure 3. Temperature dependence of the ^{1}H NMR Spectrum of *cis*-[PtCl$_2$(3-bromoquinoline)(quinoline)] in dmf-d_7.

The complex *cis*-[PtCl$_2$(3-bromoquinoline)(quinoline)] was prepared to alleviate the symmetry-imposed absence of inter-ring H2/H2 and H8/H8 cross-peaks in the NOESY spectrum of *cis*-[PtCl$_2$(quinoline)$_2$] because the Br substituent on one of the rings renders the two rings inequivalent. The 3-position of the bromo grouping was chosen so that the greater steric bulk of Br over H did not seriously affect the rotational energy barrier about the Pt−N bond.

Variable-Temperature ^{1}H NMR. A series of ^{1}H NMR spectra of *cis*-[PtCl$_2$(quinoline)$_2$] and *cis*-[PtCl$_2$(3-bromoquinoline)(quinoline)] were recorded in dmf-d_7 in the temperature range 215−370 K (Figures 2 and 3). The spectra display small changes in the chemical shifts of some resonances between 215 and 295 K, and the peaks broaden and then coalesce as the temperature is raised through the range 315−335 K for both complexes. For *cis*-[PtCl$_2$(quinoline)$_2$], two sets of resonances are observed at lower temperatures due to the two forms (HTT and HTH) (Scheme 1). At higher temperatures one averaged set of resonances is observed indicating that conformational exchange between forms is occurring on the NMR time scale. For *cis*-[PtCl$_2$(3-bromoquinoline)(quinoline)] at lower temperature four sets of quinoline resonances are observed (two for both quinoline and 3-bromoquinoline) and these merge as the temperature is raised. No clearly defined single set of peaks for a completely averaged conformation was observed for *cis*-[PtCl$_2$(3-bromoquinoline)(quinoline)] as the temperature was not raised above 370 K.

A line shape analysis of the temperature dependence of the ^{1}H spectra of both complexes was carried out, using the shifts

(39) *HYPERCHEM*, 4.5 for windows ed.; HyperCube, 1995.
(40) Hambley, T. W. *J. Comput. Chem.* **1987**, *8*, 651−657.
(41) *Atlas of Spectral Data and Physical Constants for Organic Compounds*; CRC Press: Cleveland, OH, 1973.

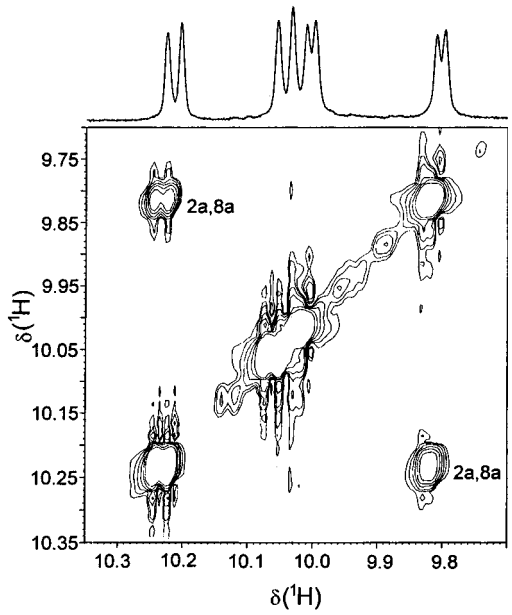

Figure 4. NOESY NMR spectrum of *cis*-[$PtCl_2$(quinoline)$_2$] at 215 K in dmf-d_7 showing the H2/H8 cross-peaks.

and line widths of the H8 protons of the quinoline ring at a temperature where there was no exchange between rotamers, and the data were subjected to an Arrhenius analysis giving rotational energy barriers about Pt−N of 82 ± 4 kJ mol^{-1} for *cis*-[$PtCl_2$(quinoline)$_2$] and 79 ± 5 kJ mol^{-1} for *cis*-[$PtCl_2$(3-bromoquinoline)(quinoline)].

The ^{1}H NMR spectra indicate two sets of quinoline resonances at low temperature becoming one set of quinoline resonances at higher temperatures. The observation of only one set of NOESY cross-peaks (vide infra) at low temperature indicates that the species are symmetric, and therefore, we can conclude that there are two symmetric species each of which gives rise to one set of quinoline resonances. On exchange, resonances due to the two symmetric species become averaged giving a single set of quinoline resonances.

NOESY Spectra. Conformational exchange between the two rotamers of *cis*-[$PtCl_2$(quinoline)$_2$] occurs on the NOESY NMR time scale at 295 K. At 215 K, no exchange between the two rotamers is observed in the NOESY spectrum (Figure 4). For *cis*-[$PtCl_2$(quinoline)$_2$] two sets of quinoline peaks are observed at 215 K. The HTH isomer would give rise to one set of quinoline resonances. Similarly, the HTT isomer would give one set of resonances due to the protons of the quinoline rings. In the case of the HTT rotamer, inter-ring H2/H8 NOESY cross-peaks are observed (Figure 4). In the case of the HTH rotamer, no H2/H2 or H8/H8 cross-peaks can be observed (by equivalence) (Figure 4), and no H2/H8 cross-peak would be expected.

The ^{1}H NMR spectra of *cis*-[$PtCl_2$(3-bromoquinoline)(quinoline)] show that two conformational forms are present, based on assignment of 25 resonances due to quinoline protons. The two conformers give rise to two sets of resonances of approximately equal intensity, indicating that the Br substituent has negligible effect on the energy difference between the two conformational forms (vide infra). This is in agreement with the COSY and NOESY NMR spectra recorded at 240 K, at which no interconversion occurred. NOESY cross-peaks were not observed between all H2 and H8 resonances, discounting the possibility that rapid interconversion is occurring between conformers. The NOESY spectrum shows cross-peaks between the H2/H2′, H2a/H8′a, and H8/H8′ resonances (Figure 5). The expected cross-peak between H2′a/H8a could not be resolved

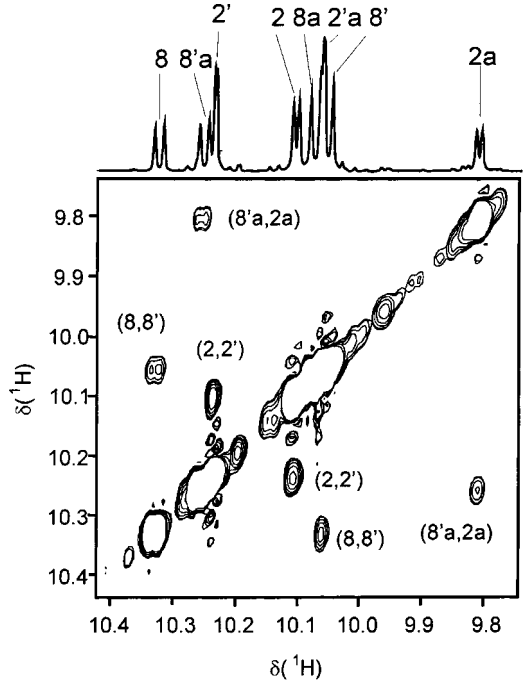

Figure 5. NOESY NMR Spectrum of *cis*-[$PtCl_2$(3-bromoquinoline)-(quinoline)] at 240 K in dmf-d_7 showing the H2a/H8′a, H2/H2′, and H8/H8′ cross-peaks.

Table 3. Minimized Strain Energies (kJ mol^{-1})

complex	HTT	HTH	Δ*E*
cis-[$PtCl_2$(quinoline)$_2$]	19.8	21.4	1.6
cis-[$PtCl_2$(3-bromoquinoline)(quinoline)]	18.1	19.8	1.7
cis-[$PtCl_2$(3-bromoquinoline)$_2$]	16.3	18.0	1.7

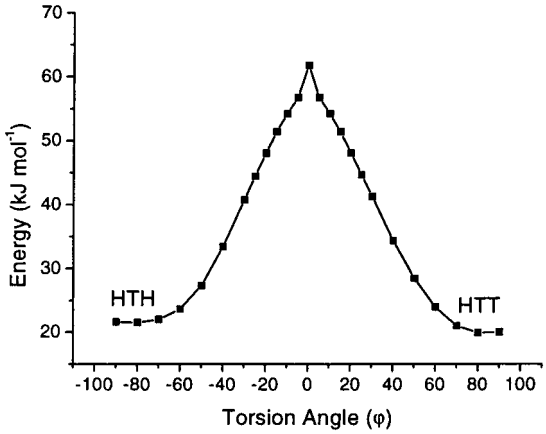

Figure 6. Plot of strain energy as a function of the torsion angle (φ) for *cis*-[$PtCl_2$(quinoline)$_2$].

from the diagonal. Observation of the H2/H2′ and H8/H8′ cross-peaks as well as the H2a/H8′ cross-peaks indicates that both the HTH and HTT forms are present for *cis*-[$PtCl_2$(3-bromoquinoline)(quinoline)]. It is reasonable to surmise that both forms are present in the bis(quinoline) complex as well.

Molecular Modeling. Models were generated for HTH and HTT rotamers of *cis*-[$PtCl_2$(quinoline)$_2$], *cis*-[$PtCl_2$(3-bromoquinoline)$_2$], and *cis*-[$PtCl_2$(3-bromoquinoline)(quinoline)]. Minimized strain energies are given in Table 3. Rotational energy barriers were estimated by using constraints on N−Pt−N−C torsion angles to drive the quinoline ligands from one orientation to the other. Strain energy plotted as a function of the rotation angle is shown in Figure 6, and this was used to obtain a lower limit for the rotational energy barrier.

Table 4. Nonbonded Distances (Å) between Quinoline Ligands in *cis*-[$PtCl_2$(quinoline)$_2$] and *cis*-[$PtCl_2$(3-bromoquinoline)(quinoline)] from X-ray Crystal Structural, NOESY NMR Spectral, and Molecular Mechanics Analysis

	HTH			HTT		
atoms	X-ray[a]	mol mech[a]	NOESY[b]	X-ray[a]	mol mech[a]	NOESY[b]
H2···H2	2.36	2.60	2.17			
H8···H8	2.60	2.42	2.35			
H2···H8[a]				2.54	2.67	2.41
H2···H8[b]						2.51

[a] Data refer to *cis*-[$PtCl_2$(quinoline)$_2$]. [b] Data refer to *cis*-[$PtCl_2$(3-bromoquinoline)(quinoline)].

Discussion

The bis(quinoline)platinum(II) complexes in this study were selected because they are free of complicating interactions such as hydrogen bonds and therefore the underlying factors influencing rotamer geometry, distribution, and interconversion can be determined. The three techniques employed provide information on the equilibrium geometries of the complexes, the relative stabilities of the HTT and HTH rotamers observed, and the barrier to interconversion of these isomers. The only substantial degrees of freedom in these complexes are the rotation angles about the Pt−N(quinoline) bonds, and these are reflected in the separations between the H2 and H8 atoms lying on the periphery of the ligands.

Equilibrium Geometries. The distances between H atoms of the two quinoline rings in the HTH and HTT forms of both complexes determined crystallographically, from NOESY cross-peak intensities, and from the molecular mechanics models are summarized in Table 4. The inter-ring distances between the H2 and H8 nuclei were estimated from the intensities of the H2/H8 cross-peak for *cis*-[$PtCl_2$(quinoline)$_2$] and *cis*-[$PtCl_2$(3-bromoquinoline)(quinoline)], using the intensity of a vicinal H3/H4 cross-peak and a distance between these two nuclei of 2.37 Å as a reference, to be 2.41 and 2.51 Å, respectively (see Table 4). These distances are in good agreement with the distances found in the X-ray crystal structure for the HTT form of *cis*-[$PtCl_2$(quinoline)$_2$] of 2.54 Å but all are less that the molecular mechanics value of 2.67 Å. The increased mobility of the ligands in solution may account for differences between distances found by X-ray diffractometry and those from NOESY spectra, the latter known to be dependent on mobility and therefore less precise.[42−44] Comparison of the molecular mechanics and crystal structure geometries shows differences in the canting angles about the Pt−N(quinoline) bonds which are 75−77° in the solid state and 82° in the molecular mechanics models. This difference is responsible for the H2···H2 separation being the longer in the molecular mechanics model and H8···H8 being the longer in the solid state. These canting angles are likely to be affected by crystal packing and solvent interactions. No estimate can be made of the H2/H2 or H8/H8 distances for the HTH form of *cis*-[$PtCl_2$(quinoline)$_2$] in solution, but for *cis*-[$PtCl_2$(3-bromoquinoline)(quinoline)] the H8/H8 distance of 2.35 Å and the H2/H2 distance of 2.17 Å are shorter than the distances in the crystal structure and molecular mechanics model of 2.36−2.60 Å. The 2.17 Å separation is extremely short, being a strongly repulsive H···H interaction. The shorter H2/H2 distances determined in solution could be attributed to the flexibility of the molecule in solution or the greater imprecision of the internuclear distance determination in solution. Molecular mechanics calculations show that the Br makes no close contacts and does not significantly influence the equilibrium geometry.

Isomer Distributions. In all cases the strain energies calculated for the HTH and HTT rotamers differ by only ∼2 kJ mol^{-1}. Thus, on the basis of the molecular mechanics calculations, approximately equal amounts of the two rotamers would be expected. The similarity of the intensities of the NMR peaks arising from the individual rotamers is consistent with their having similar stabilities as is the observation of both rotamers in the solid state. The lack of significant interligand repulsions between the quinoline ligands also leads to the expectation that neither rotamer will be preferred over the other.

Rotational Energy Barrier. Interconversion from one rotamer to the other involves rotation about a Pt−N(quinoline) bond in the direction that results in a close contact between H8 of one quinoline ligand and either a chloro ligand or the N(quinoline) atom of the other quinoline ligand. Manipulation of unminimized molecular models shows that the close contacts that arise during rotation are H8···Cl (∼1.26 Å) or the H8···N(quinoline) of the other quinoline ligand (1.1 Å). These close nonbonded interactions and the accompanying electrostatic repulsions are likely to be major contributors to the energy barrier to rotation. Direct comparison with cisplatin or Pt(amine) molecules is limited as the electrostatic interactions between an NH_3 group and a chloro ligand with the aromatic quinoline ligands will differ. The rotational energy barrier for *cis*-[$PtCl_2$(quinoline)$_2$] about Pt−N was found to be 82 ± 4 kJ mol^{-1} and for *cis*-[$PtCl_2$(3-bromoquinoline)(quinoline)] was 79 ± 5 kJ mol^{-1}. This value is in good agreement with the rotational energy barrier (of ∼70 kJ mol^{-1}) determined by Bose[20] for 6-aminopurine derivatives of Pt(II) and with Stang et al.[21] in their study of [Pt(quinoline)$_2$(PEt_3)$_2$](OTf)$_2$ (OTf = triflate) (>70 kJ mol^{-1}) and Rochon et al.[22] of >71 kJ mol^{-1} on *trans*-[$PtCl_2$(2-methylpyridine)$_2$].

The barrier to rotation about Pt−N(quinoline) estimated using molecular mechanics models is about 40 kJ mol^{-1} (Figure 6), some 40 kJ mol^{-1} lower than the energy barrier determined experimentally. Closely related force fields were successful in reproducing the barriers to rotation about Pt−N7(purine) bonds,[9] but in those cases where there were large barriers, they were steric in origin. Here it is clear that the steric barrier is substantial but may not be sufficient to account for the experimentally observed barrier. It may be that there is an electronic barrier to rotation about the Pt−N(quinoline) bond, and some support for this suggestion comes from a DFT study of Pt(II)/pyridine systems. Preliminary results of these DFT calculations give a barrier of about 26 kJ mol^{-1} to rotation about the Pt−N(pyridine) bond.[45] Using the same force field as that used here a steric barrier to rotation about a Pt−N(pyridine) bond of about 15 kJ mol^{-1} is calculated[45] consistent with an electronic barrier of about 10 kJ mol^{-1}. However, an electronic component of this magnitude would not account for the difference between observed and calculated barriers in the *cis*-[$PtCl_2$(quinoline)$_2$] system. Another factor may be the large distortion of the coordination sphere in the transition state. Our models use 1,3 -interactions in the coordination sphere, and although these are effective in modestly distorted systems, they may not, on their

(42) Wuthrich, K. *NMR of proteins and nucleic acids*; Wiley-Interscience: New York, 1986.
(43) Luxon, B. A.; Gorenstein, D. G. *Methods Enzymol.* **1995**, *261*, 45−73.
(44) Braun, W.; Bosch, C.; Brown, L. R.; Go, N.; Wuthrich, K. *Biochim. Biophys. Acta* **1981**, *667*, 377−396.
(45) Toh, J.; Bacskay, G. B.; Davies, M. S.; Hambley, T. W. Unpublished results.

own, be adequate to model highly distorted systems. Molecular mechanics and DFT studies are underway to investigate further the origins of the rotation barriers.

Acknowledgment. The authors wish to thank Dr. Ian Luck for assistance with NMR experiments and simulations. The support of the Australian Research Council is gratefully acknowledged.

Supporting Information Available: Tables of crystal data, positional and thermal parameters, bond lengths and angles, and least-squares planes, complete low-temperature NOESY spectra of *cis*-[$PtCl_2$(quinoline)$_2$] and *cis*-[$PtCl_2$(3-bromoquinoline)(quinoline)], and the NOESY spectrum of *cis*-[$PtCl_2$(quinoline)$_2$] at 300 K. This material is provided free of charge via the Internet at http://pubs.acs.org.

IC001278V